12

. . . . . contributing to man's
understanding of the environment World

TECHNICAL REPORT NO. 84-3
FINAL REPORT ON THE
MODEL 44000 SEISMOMETER SYSTEM DEVELOPMENT

SPONSORED BY
DEFENSE ADVANCED RESEARCH PROJECTS AGENCY (DOD)
DARPA ORDER NO. 3328

RELEASE AUTHORIZATION

APPROVED FOR PUBLIC RELEASE, UNLIMITED DISTRIBUTION

TELEDYNE GEOTECH

TECHNICAL REPORT NO. 84-3

FINAL REPORT ON THE

MODEL 44000 SEISMOMETER SYSTEM DEVELOPMENT

Sponsored by

Defense Advanced Research Projects Agency (DOD)

DARPA Order No. 3328

ACKNOWLEDGEMENT

This research was supported by the Advanced Research Projects Agency of the Department of Defense and was monitored by AFTAC/TGX, Patrick AFB, FL 32925, under Contract No. F08606-78-C-0034

RELEASE AUTHORIZATION

Approved for public release, unlimited distribution

DISCLAIMER

The views and conclusions contained in this document are those of the authors and should not be interpreted as necessarily representing the official policies, either expressed or implied, of the Advanced Research Projects Agency, the Air Force Technical Applications Center, or the U. S. Government.

Teledyne Geotech
3401 Shiloh Road
Garland, Texas 75041

23 October 1984

337/250

CONTENTS

ILLUSTRATIONS

SUMMARY

This report describes the work accomplished under Contract F08606-78-C-0034, entitled Model 44000 Seismometer System. The contract, which was funded by the Defense Advanced Research Projects Agency, was issued and monitored by the Air Force Technical Applications Center.

It should be noted that this is the Final Report for Contract F08606-78-C-0034 and not the final report for the development. The technical development of the Model 44000 Seismometer System is not complete. Other programs at Teledyne Geotech are contributing to the development, and this report contains recommendations for continuing the development of the Model 44000 Seismometer System.

The purpose of the project was to develop a new borehole seismometer system that has a lower life-cycle cost, but has performance characteristics that are equal to or better than the Teledyne Geotech Model KS36000 Seismometer System. Since the cost of the borehole is a major part of the installed cost of the Model KS36000 system, the approach recommended for the Model 44000 system was to incorporate designs that would make it possible to reduce the cost of boreholes by relaxing the borehole verticality constraints from 5 degrees to 15 degrees and reducing the required borehole diameter from not less than seven inches to not less than four inches. To accomplish these objectives, new system designs containing the following general features were developed:

- Sensor module support through their geometrical centers to provide the space required to tilt them up to 15 degrees from the vertical

axis of the sensor package.

- Reduced sensor module diameter to provide an overall package diameter of 3-3/4 inches.

A second objective of the program was to provide design improvements that would overcome deficiencies that were known to exist in the Model KS36000 system. These included more rugged mass suspensions to reduce the possibility of damage caused by rough handling and force feedback through the center of mass to eliminate electromechanical resonances in the suspensions.

The scope of the development program included the design of the seismometer package plus associated peripheral equipment including the holelock, holelock installation tool, the stabilizer, the cable strain relief, the cable assembly including connectors, signal conditioning circuits, seismometer controller, and the wellhead terminal.

The designs for the peripheral equipment were straightforward versions of the KS36000 designs and were completed through test and evaluation without difficulty. Most of the technical effort on the contract was directed toward the design and evaluation of the sensor modules. In order to achieve satisfactory module performance, it was necessary to maintain a high-level, long-term vacuum within the modules. Paragraphs 3.0 and 4.1 of the technical report discuss the requirements for high vacuums and outline the steps taken to meet this requirement. The vacuum problem was solved, and the results of tests with leak detectors and measurement of mechanical Q of the suspensions indicate a module life in excess of ten years.

An important design objective was to place the feedback force vector through the center of the suspended mass to prevent electromechanical resonance in the suspension. A decision was made to use electrostatic feedback to the sensor primary capacitor plates. Section 3 of the report contains a discussion of the rationale followed in the development effort. The conclusion reached in evaluating the equations for the closed-loop suspension was that the inherent nonlinearities in an electrostatic feedback system could be overcome through the appropriate selection of circuit parameters. The vertical and horizontal modules were designed, and models were built and tested using electrostatic feedback. Tests in Geotech's borehole test facilities in Garland revealed that system noise exceeded the predicted level by about 20 dB. To determine the cause, a detailed analysis of the loop circuit equations was conducted, and it was determined that there is not a set of circuit parameters that will satisfy the requirements for both loop circuit response and linearity. An analysis of the loop circuit equations is given in Appendix B. It was concluded that the system noise was caused by nonlinearities in the feedback system. At that time, Geotech recommended that an inherently linear electromagnetic feedback transducer be used instead of the electrostatic transducer.

The Model 44000 modules are supported on spherical surfaces centered around the center of mass of the module. It was not feasible to use an air bearing for leveling as is done in the Model KS36000, so a leveling table was developed to move (tilt) the module to any position within a 15-degree cone.

The method of leveling involves the use of a microprocessor-based controller to drive the table. The controller solves a series of trigonometric

equations to find the module position in which the mass is centered and the capacitance bridge is balanced. Two controller designs were developed. The first design was found to require considerable operator skill, and it was concluded that the method should be simplified so that special training and operator proficiency was not required. The second approach has been designed, coded and burned into the microprocessor PROM, but has not been tested in a seismometer system. This leveling program will result in essentially automatic leveling, and it will be possible for an operator to read the instructions and level the seismometer modules without difficulty.

Section 5 of the report shows data from tests conducted at the Garland borehole test facility. In these tests, the performance of the Model 44000 seismometer is compared with a Model KS36000 seismometer. The systems were installed in adjacent boreholes. The results, which are discussed in Section 5 of the report, show that the performance of the Model 44000 compares very favorably with that of the Model KS36000 system. Coherence plots show good coherence in the short-period passband. Test results show that some system noise exists in the long-period passband of the Model 44000 vertical channel (Figure 5-4). Teledyne Geotech believes that this noise is caused by nonlinearities in the electrostatic feedback and that it will be eliminated by changing to an electromagnetic feedback transducer.

Since the contract funds were depleted in early 1983, Geotech has continued efforts on the system development. Accomplishments include, among other things, design modifications for the electromagnetic transducer and revisions to the software system for the leveler controller. The work remaining to be

done is to modify the two Model 44000 systems that belong to the Government and to conduct the comparative testing required to verify that the current designs will meet the specified performance requirements.

1. INTRODUCTION

In fiscal year 1978, the Defense Advanced Research Projects Agency (DARPA) funded Contract F08606-78-C-0034, entitled Model 44000 Seismometer System. This contract was funded in response to an unsolicited proposal (P-2928) which Teledyne Geotech submitted to DARPA through the Air Force Technical Applications Center (AFTAC) office at the VELA Seismological Center. The work was proposed to be accomplished in three phases: I - System Development, II -Prototype Production, and III - Performance Testing and System Documentation. Prior to submitting the proposal, Teledyne Geotech had designed, fabricated, and conducted preliminary testing of two horizontal seismometer modules. Design concepts had also been developed for a vertical module. The program was planned to cover a total of 40 months and to be completed in November 1982. During the course of this contract, technical difficulties caused budget and schedule problems, and, in November 1982, the work had not been completed. Funding authorized in 1983 was limited to $12,500, so only a small amount of contractual effort was accomplished. Geotech did, however, make significant progress in developing software for the leveler control subsystem and in modifications to change the sensor feedback from electrostatic to electromagnetic.

This report is submitted in compliance with the Contract Data Requirements List Item 00F/A2 and is the final report for the contract.

2. PURPOSE OF THE PROGRAM

During the early 1970's, Teledyne Geotech developed designs for a high-quality, long-period seismograph system using concepts that made it possible to provide small transducers that could be packaged for use in small-diameter boreholes. After Geotech demonstrated design feasibility, DARPA provided funds through AFTAC's Seismic Data Collection System (SDCS) program to develop packaging concepts for a system to be installed in a seven-inch, cased borehole. The system became known as the Teledyne Geotech Model KS36000 seismometer system. Additional DARPA funds were provided to manufacture a number of systems for use in the United States Geological Survey (USGS) Seismic Research Observatory (SRO) program, for the SDCS program, and support research under the direction of the Air Force Office of Scientific Research. These systems were delivered to the various government organizations by the end of 1975, and the technical objectives were met or exceeded in all respects. The system was designed to be installed in a cased borehole not more than 5° off vertical, and it turned out that such verticality was difficult to achieve in practice. The cost for boreholes became a significant part of the installed cost for a KS36000 system. In 1976 and 1977, Teledyne Geotech funded a program to develop design concepts that would make it possible to relax the verticality requirements. As a result of this effort, a new sensor system design was developed for boreholes as much as 15° off vertical. A contract was awarded to Geotech in July 1978, and development effort was started in August 1978.

The objective of the program was to design a borehole system having overall performance that matched or exceeded that of the KS36000 system, but which

had an installed cost significantly less than that for the KS36000. New technology that could contribute to reduced manufacturing cost and improved reliability was to be considered in the development program.

3. THEORETICAL BASIS

In considering ways to reduce the installed cost of long-period borehole seismometer systems, Geotech first concluded that it was not likely that significant cost reductions could be realized in the seismometer design itself. This left the cost of the borehole the remaining major cost factor. Borehole cost could be reduced by: 1) reducing the borehole diameter and, thus, making it possible for smaller, less-expensive and more-mobile drill rigs to be used; and 2) to relax the borehole verticality requirements to the point that, in most cases, verticality constraints would not be a risk factor in estimating the cost of a borehole. Geotech first considered design changes in the KS36000 seismometer, but concluded that changes to reduce the diameter or to relax the verticality constraints would require engineering effort equivalent to that of developing a new design. Also, Geotech believed that if a new design approach was undertaken, a more rugged suspension could be developed and thus overcome another recognized shortcoming of the KS36000 system. It was at this point that Geotech decided to develop the designs for the Model 44000 seismometer system. The key design objectives for the system were:

- Match or exceed the performance of the KS36000 system;
- Cost not to exceed that of the KS36000 system;
- Design for installing in a 4-inch inside diameter (4½ inch American Petroleum Institute casing) borehole up to 15° off vertical;
- Design to reduce the complexity of installation, operation, and maintenance procedures;
- Take maximum advantage of design concepts already developed for the KS36000 system.

The designs that evolved after a number of studies were a simple pendulum for the horizontal module and a simple spring-mass system for the vertical. These designs enabled Geotech to develop more rugged suspensions because their natural frequencies were about 2.2 hertz (Hz) (the KS36000 is 0.2 Hz). Geotech was also able to design in-limit stops to prevent overstress in the suspensions due to shocks caused by rough handling.

In the theory of the design of these inertial sensors (Melton, 1976), the limiting noise at the system output is in the damping force applied from the frame to the inertial mass (M) x the natural period (P) x quality (Q) of the inertial suspension. An objective in the 44000 program was to achieve an MPQ product that was equal to or greater than that of the KS36000. The mass in the 44000 is 200 grams versus 370 grams in the KS36000, and its natural period is 0.4 second versus 5 seconds in the KS36000. Thus, the mechanical Q must be at least 23 times greater in the 44000 suspension than it is in the KS36000. High mechanical Q's cannot be achieved in the presence of air, so the suspension must be operated in a vacuum.

Other design features in the Model 44000 system include module support through their centers of gravity to reduce the possibility of damage caused by rough handling, suspension feedback force through the center of mass to prevent spurious modes in the suspension, and mass travel limited to about 50 microns, thus eliminating the need for mass locks.

The design of the Model 44000 suspension is configured to have two parallel plate capacitors in which the mass is a common plate between two outer plates as illustrated in the diagrams of the horizontal module in figure 3-1. The use of electrostatic feedback for the system was investigated because the

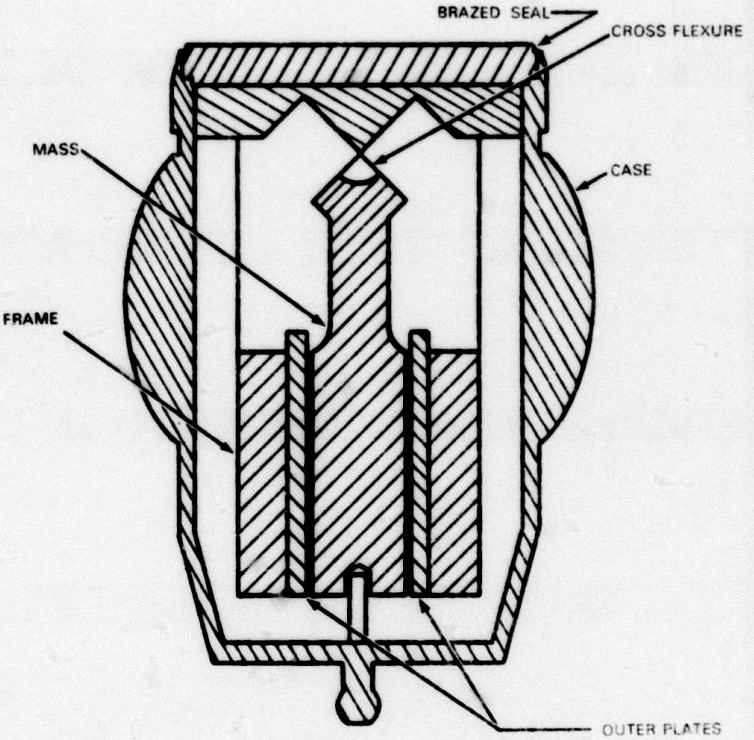

FIGURE 3-1 a. SCHEMATIC REPRESENTATION OF THE MODEL 44000 HORIZONTAL SUSPENSION

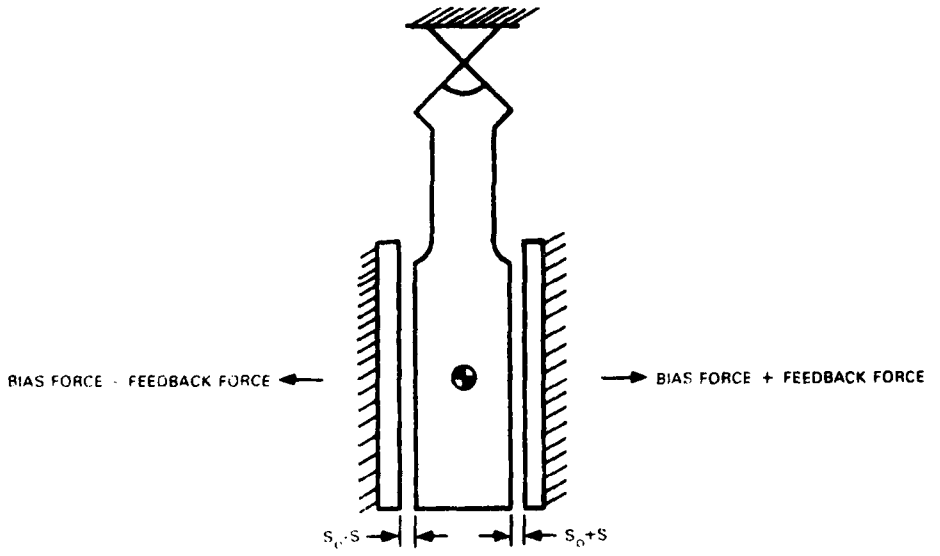

FIGURE 3-1 b. ELECTROSTATIC FEEDBACK THROUGH THE CENTER OF MASS

mechanical design was less complex than it would be if an electromagnetic transducer had to be added to the suspension. It was known that the electrostatic feedback had nonlinear properties, so the equations for a parallel plate capacitor were developed and studied. The nonlinear terms in the resulting equation were

$$N = \left(2 - \frac{G}{V_o}\right)\left(\frac{S}{S_o}\right)^2 + \left(3 - 2\,\frac{G}{V_o}\right)\left(\frac{S}{S_o}\right)^4$$

Where G is the feedback loop gain, V_o is the bias voltage, and $S_o - S$ and $S_o + S$ are the plate spacings in the two capacitors. The derivation for the equation is included in appendix 1. Note that if $G/V_o = 2$, the squared term goes to zero, and, for $S \ll S_o$, the fourth-power term becomes negligible. Electrostatic feedback was selected on the basis of this analysis. Subsequent problems with sensor nonliniarites are discussed in section 4, Technical Problems.

4. TECHNICAL PROBLEMS

In the original contract, the plan called for fabricating and testing an engineering model of the 44000 system in twelve months (Phase I). The engineering model was completed; however, technical difficulties prevented completion of testing. The following paragraphs contain discussions of the important problems encountered.

4.1 MODULE VACUUM

One of the first significant problems was that of maintaining a vacuum within the modules. To maintain a mechanical Q in excess of 1000, it was necessary to achieve a vacuum of less than 1 milli-torr, maintain a leak rate not to exceed 5×10^{-12} Standard cubic centimeters per minute (Std cc/min), and have a very low level of outgassing within the module. Since the volume of the 44000 modules is much smaller than that of the 36000, outgassing in the 44000 had to be significantly less in volume. The required vacuum was achieved by baking at about 250°F during pumpdown. This required pumpdown periods of two to four weeks to achieve the required vacuum. Q's of more than 10,000 were achieved, but they dropped below 1000 in a period of two or three weeks. As part of the effort to resolve this problem, Dr. John Hoffman at the University of Texas at Dallas, a recognized expert in long-term vacuum technolgy, was consulted. After reviewing Geotech's design, Dr. Hoffman recommended that the O-ring seal in the cover be eliminated and that the cover be brazed rather than soldered. He also recommended the use of ceramic-encapsulated feedthroughs rather than glass. These design modifications were made, and tests indicated that the seal problem had been solved. Figure 4-1 illustrates the before and after seal designs. Tests indicated that the new seal design could be expected to reduce the leak rate to

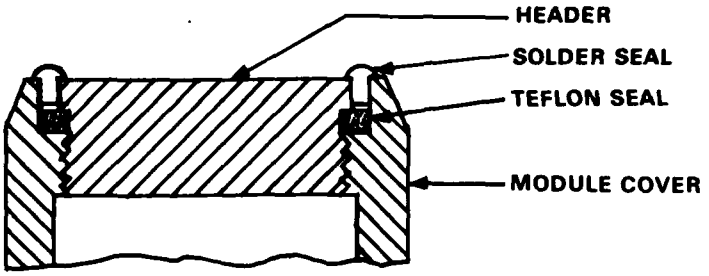

ORIGINAL DESIGN. SOLDER FLUX AND OTHER CONTAMINANTS CAN BE TRAPPED BETWEEN SOLDER SEAL AND TEFLON SEAL, PRODUCING A SOURCE FOR OUTGASSING AFTER BAKE-OUT.

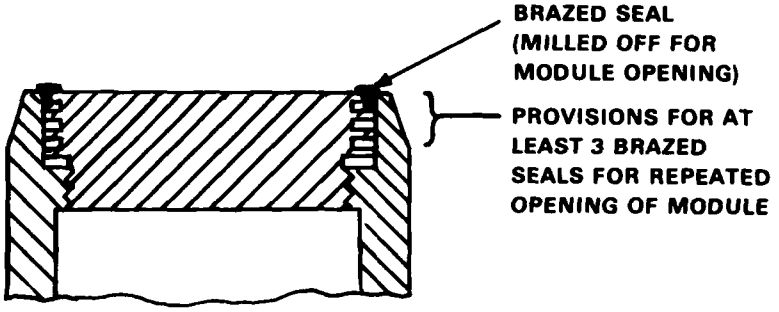

PRESENT DESIGN. HIGH-TEMPERATURE BRAZED SEAL ALLOWS BAKE-OUT AT HIGHER TEMPERATURE TO REMOVE ANY FLUX OR CONTAMINANTS WHICH HAVE BEEN TRAPPED BEHIND THE BRAZED SEAL.

Figure 4-1. 44000 Seismometer Module Vacuum Seal

G14916

about 4 x 10^{-13} Std cc/min corresponding to a module life greater than twelve years.

4.2 MASS FLEXURE DESIGN

In the early design efforts, geotech estimated that it would not be possible to achieve a mechanical Q much greater than about 1000, so the suspensions were designed to have natural periods of about .45 second (2.2 Hz). These suspensions were relatively rugged, but, after much higher Q's than expected were observed, stiffer flexures were placed in the modules, and the natural period was decreased to 0.4 second (2.5 Hz). This made the suspensions less susceptible to damage.

4.3 MODULE LEVELING

A design objective was to reduce the skill level required to install and operate the seismometer. A major step in this direction was to provide a means for automatic leveling from a control system to be used at the wellhead. This turned out to be a much more complex problem than had been anticipated. The leveling algorithm was implemented in a rather large software program in a microcomputer. The first solution to this problem was not simple, and it took considerable training for a technician to be able to operate the leveler control system. Geotech funded the redesign of the leveler controller during late 1982 and early 1983. The software has been coded, but the program has not been fully tested in the system.

4.4 SYSTEM NOISE

Tests conducted during October 1978 indicated that there was an excessive amount of incoherent noise in the system outputs that was isolated to the sensor loop electronics. At this point in the program, KS36000 loop electronic

circuits were being used, and tests revealed that new circuits were needed to reduce the 44000 system noise to an acceptable level. The design effort was completed during December 1978 and January 1979. The February 1979 monthly report stated that the new carrier source and loop electronics met the noise level requirements. Later in the program, it was found that system filters had excessive noise, but this was not a major technical issue, and the problem was corrected. System electronic noise tests conducted at that time showed that electronic noise in all parts of the system was well below expected seismic noise levels.

4.5 SYSTEM LINEARITY

After it was verified that all electronic circuits had noise levels below those required to meet system performance requirements, excessive noise was still observed in the system outputs. A great deal of effort was expended in attempts to isolate the cause of this noise. All of the spurious resonance tests were revisited; the mechanical structure supporting the modules was studied, as was the possibility of cross-feed in the system wiring; the hole-lock and stabilizer stability was tested, and numerous other tests were conducted to isolate the noise source. This effort was not successful. In the spring of 1980, the nonlinearities in the capacitor plates were studied. The results indicated that system nonlinearities could be the source of noise. A report was submitted in April 1980 which concluded that the system would have a very small nonlinear term ($1.6 \times 10^{-4}\%$) with a force bias voltage on the order of 40 volts. Tests were conducted with a 35-volt bias, but the loop circuit was not stable. At 20 volts, the loop seemed well-behaved, but resulted in a nonlinear term of 0.1%. At this point, it was decided to

proceed with the fabrication, assembly, and test of one prototype that incorporated all of the system changes that were made on the engineering model. When the prototype system was tested, it was found that system nonlinearities were seriously affecting system performance, and it was concluded that it would be necessary to change the force feedback from electrostatic to electromagnetic. Appendix B contains a report on the technical analysis of the electrostatic feedback and gives the technical justification for electromagnetic feedback. A proposal was submitted to AFTAC recommending the Model 44000 feedback be changed to elecromagnetic.

4.6 BROADBAND RESPONSE

The system linearity problems discussed in Section 4.5, System Linearity, and expanded upon in Appendix B, are interrelated with the ability to provide a broadband (0 to 4.0 Hz) response. It was determined that it was not possible to maintain the relationship $\frac{G}{V_o} = 2$ over the broadband range and at the same time produce the desired response with negligible nonlinearities. There is not a set of loop circuit component values that will produce the 4 Hz corner and at the same time meet the linearity requirements. As discussed in section 4.5, the electromagnetic feedback transducer does not have the nonlinear characteristics and the use of this linear transducer will make it possible to meet the system response requirements called for in the B-1 specification.

Blank Page

5. TECHNICAL RESULTS

This program has involved a number of complex technical problems for which there is no engineering or scientific information that can be studied for solutions. Some of the major technical issues are the behavior of materials and how they affect the ability to detect displacements of subatomic dimensions and the strange and unexplained characteristic of mechanical structures to transmit and absorb vibrational energy. Although good scientific explanations have not been developed, the program has made it possible to solve a number of the complex technical problems, and Geotech believes that it is now very close to the program's original objectives. The most important technical results that lead to this conclusion are discussed in the following paragraphs.

5.1 SYSTEM PERFORMANCE

Figures 5-1 and 5-2 contain comparative power spectral density plots for horizontal and vertical KS36000 and 44000 seismometers. These plots cover the passband from 0 to 25 Hz and were taken in the high-noise environment of Garland. The scale does not show system characteristics at frequencies below about 0.2 Hz. The plots do show very good coherence over the passband of about 0.5 to 15 Hz on both vertical and horizontal channels. These spectra illustrate that there are no spurious resonances in the 44000 system at frequencies below 15 Hz. These results are encouraging because experience has shown that it is difficult to achieve such high coherence, even with two identical systems.

Figures 5-3 and 5-4 are seismograms taken at Geotech's Garland test facility. Figure 5-3 compares the 44000 vertical (Z) and KS36000Z, each having flat

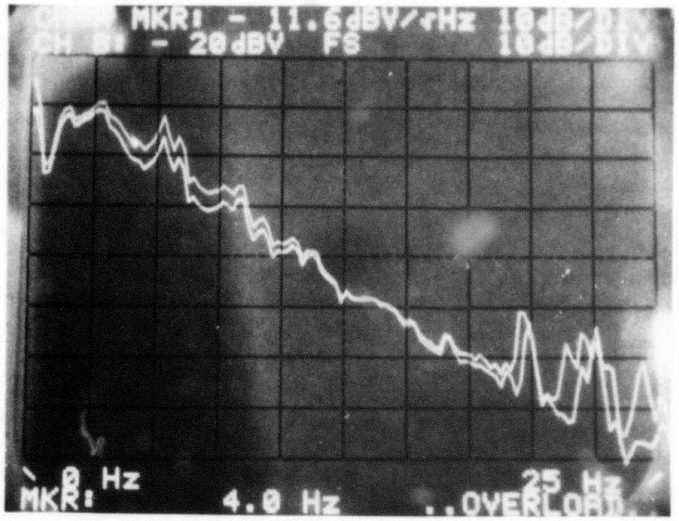

M-174

Figure 5-1a. Comparison of a KS36000 and a 44000 short-period vertical data.
Taken in Garland, Texas
Ch. A - KS36000
Ch. B - 44000
Power spectral density

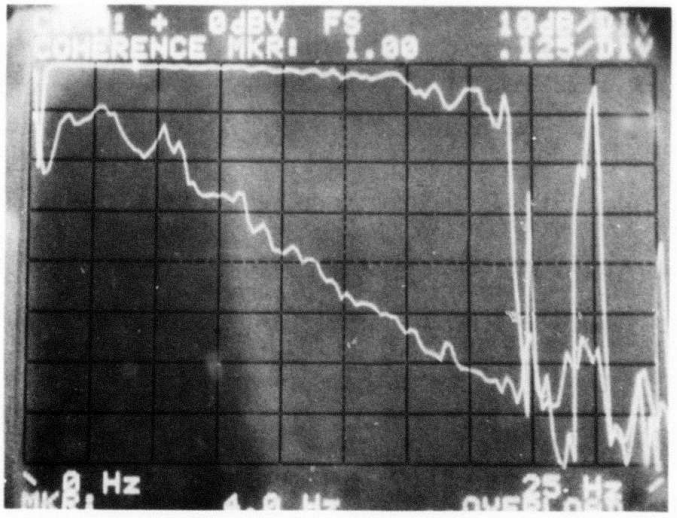

M-175

Figure 5-1b. Coherence for figure 5-1a

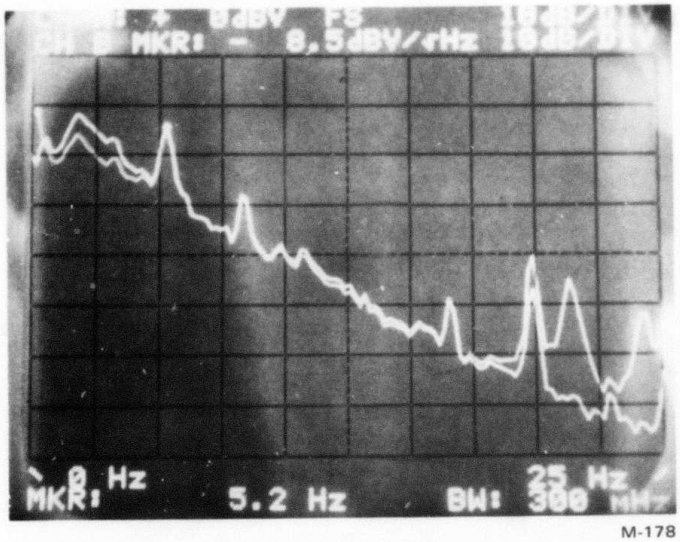

M-178

Figure 5-2a. Comparison of a KS36000 and a 44000 short-period, horizontal data. Taken in Garland, Texas

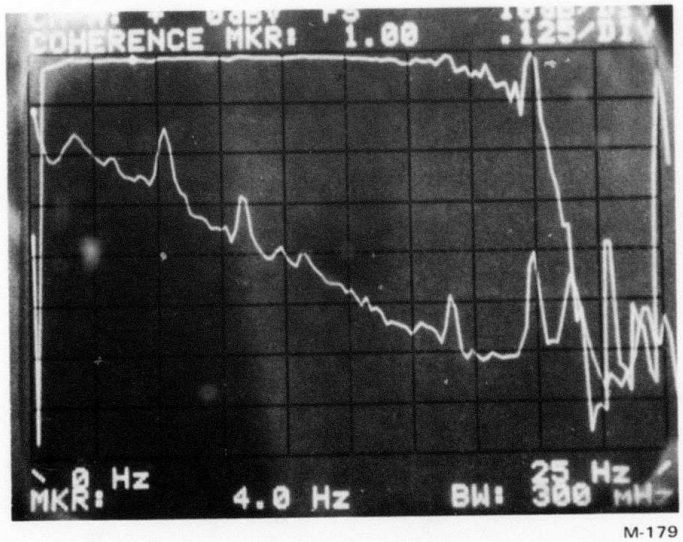

M-179

Figure 5-2b. Coherence for figure 5-2a

MODEL 44000Z - FLAT ACCELERATION, 0.001 Hz TO 4.0 Hz
MAGNIFICATION ≃ 10K AT 25 SECONDS

MODEL 44000H - FLAT ACCELERATION, 0.001 Hz TO 4.0 Hz
(TWO HORIZONTAL CHANNELS SUMMED TO FORM E-W CHANNEL)
MAGNIFICATION ≃ 10K AT 25 SECONDS

MODEL KS 36000E - FLAT ACCELERATION, 0.001 Hz TO 4.0 Hz
MAGNIFICATION ≃ 10K AT 25 SECONDS

Figure 5-3. Model 44000 and Model KS 36000 comparison, 20-second energy is from earlier surface wave arrival

G 14153

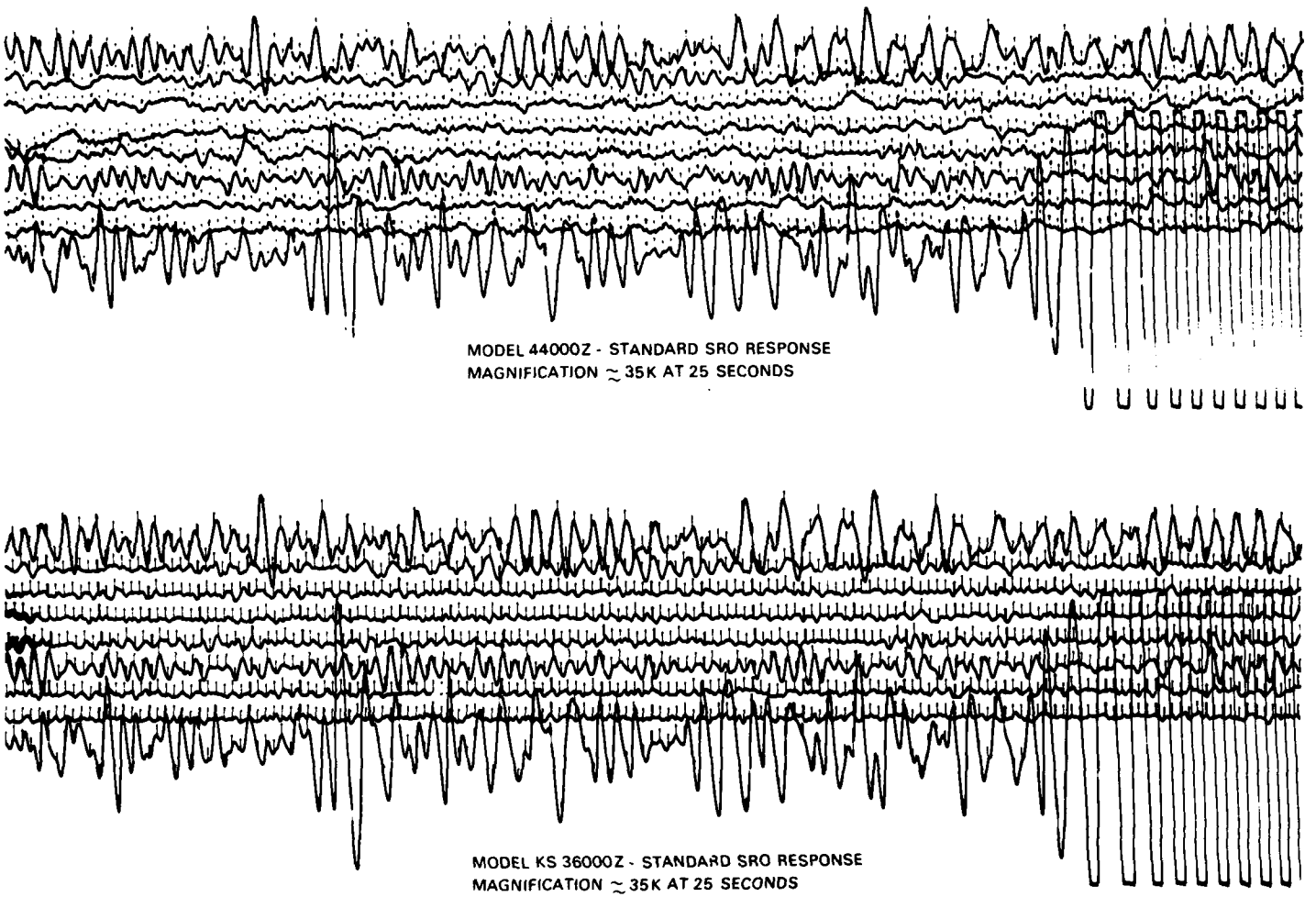

Figure 5-4. Seismogram comparing Model 44000Z and Model KS 36000Z outputs

G 14152

acceleration response over the passband from 0.001 Hz to 4 Hz. Figure 5-4 shows the two vertical channels through the standard SRO response. Note that, in figure 5-4, the systems' responses to the signals are very close to being identical, but that the 44000 record contains long-period noise that is not present on the KS36000 record. After these records were made, Mr. O. D. Starkey conducted detailed analysis and test of the 44000 loop circuits. He determined that the system parameter values used to characterize the electrostatic transducer were different from those predicted by theory. Testing also suggested that there are nonlinearities in the system. He redeveloped the equation of motion for the system without discarding any higher-order terms. The equation was very complex because of the terms required to define the electrostatic feedback circuit. These equations are included in Appendix B.

To find the solution, circuit parameters were determined by test, and their values were put into the equation. The conclusion developed from these studies were that there is not a set of parameters which will provide the desired loop response and also control the nonlinear terms. At this point, Geotech recommended to AFTAC that the electrostatic feedback system be abandoned and that the design be changed to electromagnetic feedback. Since that time, Geotech accomplished the design changes for the vertical and horizontal modules and has built engineering models for test.

5.2 LEVELER CONTROLLER

As discussed in paragraph 4.3, automatic module leveling was a rather complex problem, and the approach selected first was not a good solution because the

leveler had to start from a known position and search for the level position. The difficulty was that the system had to remember where it was relative to the initially known position if releveling was required at some later time. Also, the leveling operation could not be completed without intervention of an operator, and this required considerable skill and familiarity on the part of the operator. A new technique for accomplishing the leveling has been developed. This leveler controller determines the direction of tilt by moving each horizontal module until gravity moves the pendulum from its stop. The leveler then moves the modules on a line away from the direction of tilt until they are level. This process is automatic and does not require the attention of a skilled operator. The leveling algorithm has been coded and burned into PROM. Preliminary testing has been completed, but system-level testing has not been conducted.

5.3 STATUS OF DESIGN

All designs for the Model 44000 seismometer system are complete. Engineering models of the sensor modules with electromagnetic feedback have been fabricated on another contract and are currently being tested in the laboratory. The leveler controller design is completed up to the system-level test. Thus, all of the design effort known to be required has been done, and the next step in the program should be to modify the sensor modules and conduct laboratory and field tests.

6. CONCLUSIONS AND RECOMMENDATIONS

It is Teledyne Geotech's judgment that the Model 44000 seismometer development program is near a successful conclusion. Test results indicate that the performance of the system may exceed that of the KS36000 system because it will produce high-quality, three-component data in both the long-period and the short-period passbands. The only known critical technical issue is that of verifying that the noise observed in the last series of tests was caused by intermodulation distortion resulting from nonlinearities in the transducer loop circuit. Since electromagnetic force feedback is a linear process, the nonlinearity and, thus, the noise should be eliminated in the new module design.

It is recommended that the development program be continued and that funding be provided to accomplish the following five tasks.

Task 1: Purchase materials, fabricate parts, and incorporate all modifications in the two prototype systems. The leveler controller is installed in the latest prototype. Do not install it in the other system at this time.

Task 2: Conduct comparative borehole tests in Geotech's Garland test facilities. Write a brief report on the test results.

Task 3: Test and evaluate the leveler controller during the borehole tests called for in Task 2. Accomplish the required software debugging and update the software documentation.

Task 4: Conduct comparative borehole tests at a quiet site.

Task 5: Write a final technical report describing the work accomplished and the results of the tests.

It is recommended that Tasks 1 and 2 be completed and the results of the testing be reviewed before proceeding with Task 3. If the results of Task 2 show that the noise problem has not been eliminated, a report should be prepared describing the results and recommending whether or not the program should be continued.

7. REFERENCES

Melton, Ben S., The Sensitivity and Dynamic Range of Inertial Seismographs; Reviews of Geophysics and Space Physics, vol. 14, No. 1, p. 93-116.

APPENDIX A

EQUATIONS FOR AN IDEAL PARALLEL PLATE CAPACITOR

EQUATIONS FOR AN IDEAL PARALLEL PLATE CAPACITOR

A parallel plate capacitor with an equal, but opposite, charge (Q) on plates of area A separated by a distance d is shown in figure 1. The electric field lines are parallel, straight lines, except at the edges of the plates where fringing will occur. The ideal parallel plate capacitor assumes that the separation distance is much smaller than the linear dimensions, so that the effects of fringing are negligibly small.

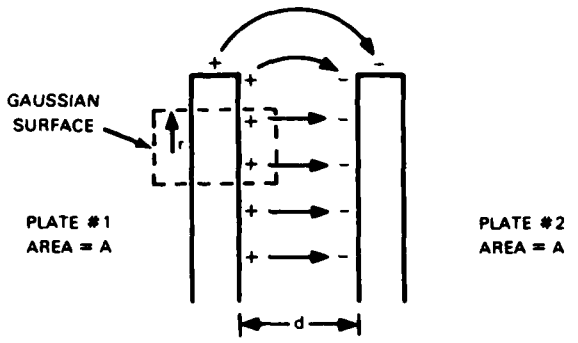

FIGURE 1. PARALLEL PLATE CAPACITOR, SHOWING FRINGING OF THE ELECTRIC FIELD AT ONE EDGE

G15023

Far enough inside the capacitor, a cylindrical Gaussian surface of radius r with its sides parallel to the field lines (as shown in figure 1) will have field lines passing through only one end of the cylinder. The flux through the Gaussian surface is then

$$\Phi = \int_S \vec{E} \cdot d\vec{s} = \pi r^2 E$$

Gauss's law states that the flux through the surface must be equal to the charge contained in the surface (divided by the permitivity constant for MKS units). The charge inside the surface is the charge density $\left(\frac{Q}{A}\right)$ times the area of the plate enclosed (πr^2)

$$\pi r^2 E = \frac{\pi r^2 \left(\frac{Q}{A}\right)}{\epsilon_o}$$

Thus, everywhere inside the capacitor,

$$E = \frac{Q}{A\epsilon_o} \qquad (1)$$

The voltage between plate two and plate one can be found from the change in potential energy

$$V = -\int_o^d \vec{E} \cdot d\vec{l} = -(-E)d$$

$$V = \frac{Qd}{A\epsilon_o} \qquad (2)$$

Using the definition of capacitance,

$$C = \frac{Q}{V}$$

$$C = \frac{A\epsilon_o}{d} \qquad (3)$$

To calculate the force on one plate, it must be noted that the field in Equation 1 must come equally from both plates. Therefore, a unit charge on one plate will have a force given by E/2 and will itself be producing the other E/2 in the gap. The force per unit charge, q, is

$$f = \frac{1}{2} qE$$

and, again neglecting edge effects, the sum over all charges gives a force on the plate of

$$F = \frac{1}{2} QE = \frac{Q^2}{2A\epsilon_o} \qquad (4)$$

$$F = \frac{A\epsilon_o V^2}{2d^2} \qquad (5)$$

TRANSDUCER OUTPUT

The output transducer is made up of two capacitors formed by the mass and two quartz plates with metallic coatings, as shown in figure 2. The circuit for obtaining a voltage output for mass displacement from the equilibrium (center) position s_o is shown in figure 3.

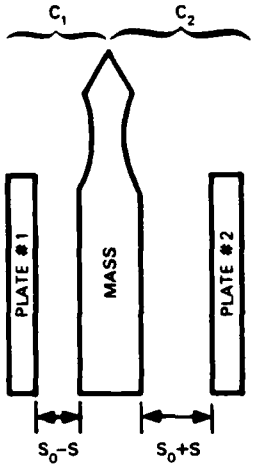

FIGURE 2. CHANGE IN CAPACITANCE C_1 AND C_2 DUE TO A DISPLACEMENT S FROM THE EQUILIBRIUM POSITION S_o.

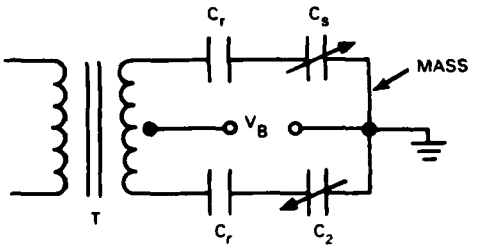

FIGURE 3. CIRCUIT FOR THE DETECTION OF CHARGES IN CAPACITORS C_1 AND C_2.

G15022

Let the voltage out of the transformer T be V_{cs}. Then, the voltage drop V_B is given by

$$V_B = \frac{1}{2} V_{cs} - I(Z_R + Z_1), \tag{6}$$

where Z is the impedance of the circuit element. Summing the voltages around the circuit loop,

$$V_{cs} = I\,(2Z_R + Z_1 + Z_2). \tag{7}$$

Solving Equation 7 for the current and substituting into Equation 6,

$$V_B = \frac{1}{2} V_{cs} - \left(\frac{Z_R + Z_1}{2Z_R + Z_1 + Z_2}\right) V_{cs} \tag{8}$$

The impedances can be evaluated using

$$Z = -iX_c \tag{9}$$

$$X_c = \frac{1}{\omega C}, \quad \omega = \text{angular frequency} \tag{10}$$

and Equation 3

$$C_1 = \frac{A\epsilon_o}{(s_o - s)} \tag{11}$$

$$C_2 = \frac{A\epsilon_o}{(s_o + s)} \tag{12}$$

$$V_B = \frac{1}{2} V_{cs} - \left(\frac{\frac{1}{C_r} + \frac{s_o - s}{A\epsilon_o}}{\frac{2}{C_r} + \frac{s_o + s}{A\epsilon_o} + \frac{s_o - s}{A\epsilon_o}} \right) V_{cs}$$

$$V_B = \frac{1}{2} V_{cs} - \left(\frac{A\epsilon_o + C_r (s_o - s)}{2A\epsilon_o + C_r(s_o - s) + C_r(s_o + s)} \right) V_{cs}$$

$$= \frac{1}{2} V_{cs} - \left(\frac{1}{2} - \frac{C_r s}{2(A\epsilon_o + C_r s_o)} \right) V_{cs}$$

$$= \frac{1}{2} V_{cs} \left(\frac{(s/s_o)}{\left(\frac{A\epsilon_o}{C_r s_o} \right) + 1} \right)$$

$$V_B = \frac{1}{2} V_{cs} \left[1 + \left(\frac{C_o}{C_r} \right) \right]^{-1} \left(\frac{s}{s_o} \right), \tag{13}$$

where $C_o = \frac{A\epsilon_o}{s_o}$ = Capacitance of C_1 and C_2 when the mass is centered.

Notice that the voltage output of the transducer circuit is directly proportional to the displacement of the mass.

FEEDBACK FORCE ON THE MASS

The force on a capacitor plate is always attractive, if the plates have equal but opposite charges. In order to exert a symmetric force on the mass, a bias voltage, V_o, is maintained on both capacitors, and a feedback voltage, V_f, is added to one and subtracted from the other. At the center position, $V_f = 0$, and no net force results. As the mass changes position, the force is increased on one side and decreased on the other so that a net force is produced. Using Equation 5, the net force is

$$F = \frac{A\epsilon_o (V_o + V_f)^2}{2(s_o+s)^2} - \frac{A\epsilon_o (V_o-V_f)^2}{2(s_o-s)^2}$$

which reduces to

$$F = \frac{2C_o}{s_o}\left[\frac{V_oV_f - (V_o^2 + V_f^2)\left(\frac{s}{s_o}\right) + V_o V_f \left(\frac{s}{s_o}\right)^2}{\left(1 - \left(\frac{s}{s_o}\right)^2\right)^2}\right] \qquad (14)$$

The feedback voltage is found from Equation 13 and

$$V_f = A V_B = G\left(\frac{s}{s_o}\right),$$

where A = transfer function of the feedback loop and

$$G = \frac{1}{2} A V_{cs}\left[\left(\frac{C_o}{C_r}\right) + 1\right]^{-1}$$

Substitution of V_f into Equation 14 results in

$$F = 4F_o \left[\frac{\left(\frac{G}{V_o} - 1\right)\left(\frac{s}{s_o}\right) + \left(\frac{G}{V_o} - \frac{G^2}{V_o^2}\right)\left(\frac{s}{s_o}\right)^3}{\left(1 - \left(\frac{s}{s_o}\right)^2\right)^2} \right] \qquad (15)$$

Where $F_o = \frac{C_o V_o^2}{2s_o}$.

Since $\left(\frac{s}{s_o}\right) << 1$, the denominator can be evaluated using the binomial expansion,

$$\left(1 - \left(\frac{s}{s_o}\right)^2\right)^{-2} = 1 + 2\left(\frac{s}{s_o}\right)^2 + 3\left(\frac{s}{s_o}\right)^4 + \ldots$$

So that

$$F = 4F_o\left(\frac{G}{V_o} - 1\right)\left[\left(\frac{s}{s_o}\right) + \left(2 - \frac{G}{V_o}\right)\left(\frac{s}{s_o}\right)^3 + \left(3 - 2\frac{G}{V_o}\right)\left(\frac{s}{s_o}\right)^5 + \ldots\right] \qquad (16)$$

Notice that the force is <u>intrinsically nonlinear</u>. In the limit as V_o approaches zero (even though it is not clear how the feedback would be applied),

$$\lim_{V_o \to 0} \{F\} = \frac{2C_o}{s_o}\left[-G^2\left(\frac{s}{s_o}\right)^3 - 2G^2\left(\frac{s}{s_o}\right)^5 + \ldots\right]$$

and there is <u>no</u> linear term. V_o has the effect of making the feedback force "more linear". In particular, it is the way in which V_o affects the ratio of higher order terms to the linear term that is of interest.

From Equation 16, the nonlinearity of the feedback force may be defined as

$$N = \left(2 - \frac{G}{V_o}\right)\left(\frac{s}{s_o}\right)^2 + \left(3 - 2\frac{G}{V_o}\right)\left(\frac{s}{s_o}\right)^4 + \ldots \qquad (17)$$

If the maximum value of s/s_o is known, then G and V_o may be changed in order to improve linearity and still maintain the same resolution and noise levels.

APPENDIX B

DETAILED REVIEW OF ELECTROSTATIC FEEDBACK FACTORS

1. INTRODUCTION

Monroe's paper entitled "Equations for an Ideal Parallel Plate Capacitor", and distributed in April 1980, represented a significant achievement in the application of electrostatic forcing transducers to feedback-controlled inertial suspensions. We do not know of any other case where the relations treated by Monroe have been recognized.

For this discussion, these unique relations are referred to as the Monroe Linearity Condition which can be concisely stated as

$$\frac{G}{V_o} = 2 \qquad (1\text{-}1)$$

where: G is the normalized gain from the output of the suspension to the input of the electrostatic forcing transducer, and

V_o is the normalized bias voltage maintained across the plates of the electrostatic transducer.

Figure 1-1 shows the functional diagram of the sensor implemented on the basis of Equation 1-1. (Notice that V_B is used here to designate the bias source voltage whereas the Monroe Paper uses V_B to designate the capacitance bridge output voltage.) The $\mathcal{F}$ designations in figure 1-1 represent the transfer functions of corresponding blocks.

Since both G and V_o in Equation 1-1 have been normalized by the transducer plate spacing s_o, we have

$$\frac{G}{s_o} = \mathcal{F}_{cs}\,\mathcal{F}_{A1}\,\mathcal{F}_{A2}\,(\mathcal{F}_{7K} + \mathcal{F}_{7V}) \stackrel{?}{=} \frac{2\,V_o}{s_o} = \frac{\text{Volts}}{\text{Meter}} \qquad (1\text{-}1a)$$

Each component in Equation 1-1a can be made constant over the frequency range of interest except $\mathcal{F}_{7V}$ which must be made frequency dependent in order to damp the closed-loop corner frequency, (4 Hz). Therefore, the closed-loop system can not satisfy Equation 1-1 over the frequency range of interest.

From April 1980 through July 1983, the sensor loop was set up on the basis of

$$\frac{G}{s_o} = \mathcal{F}_{cs}\,\mathcal{F}_{A1}\,\mathcal{F}_{A2}\,(\mathcal{F}_{7K}) = \frac{2\,V_o}{s_o} = \frac{\text{Volts}}{\text{Meter}} \qquad (1\text{-}2)$$

Since the damping component $\mathcal{F}_{7V}$ is proportional to frequency, the term $(\mathcal{F}_{7K} + \mathcal{F}_{7V})$ is dominated by the restoring component $\mathcal{F}_{7K}$ at low frequencies so that the linearity condition is approximated through the long-period data band.

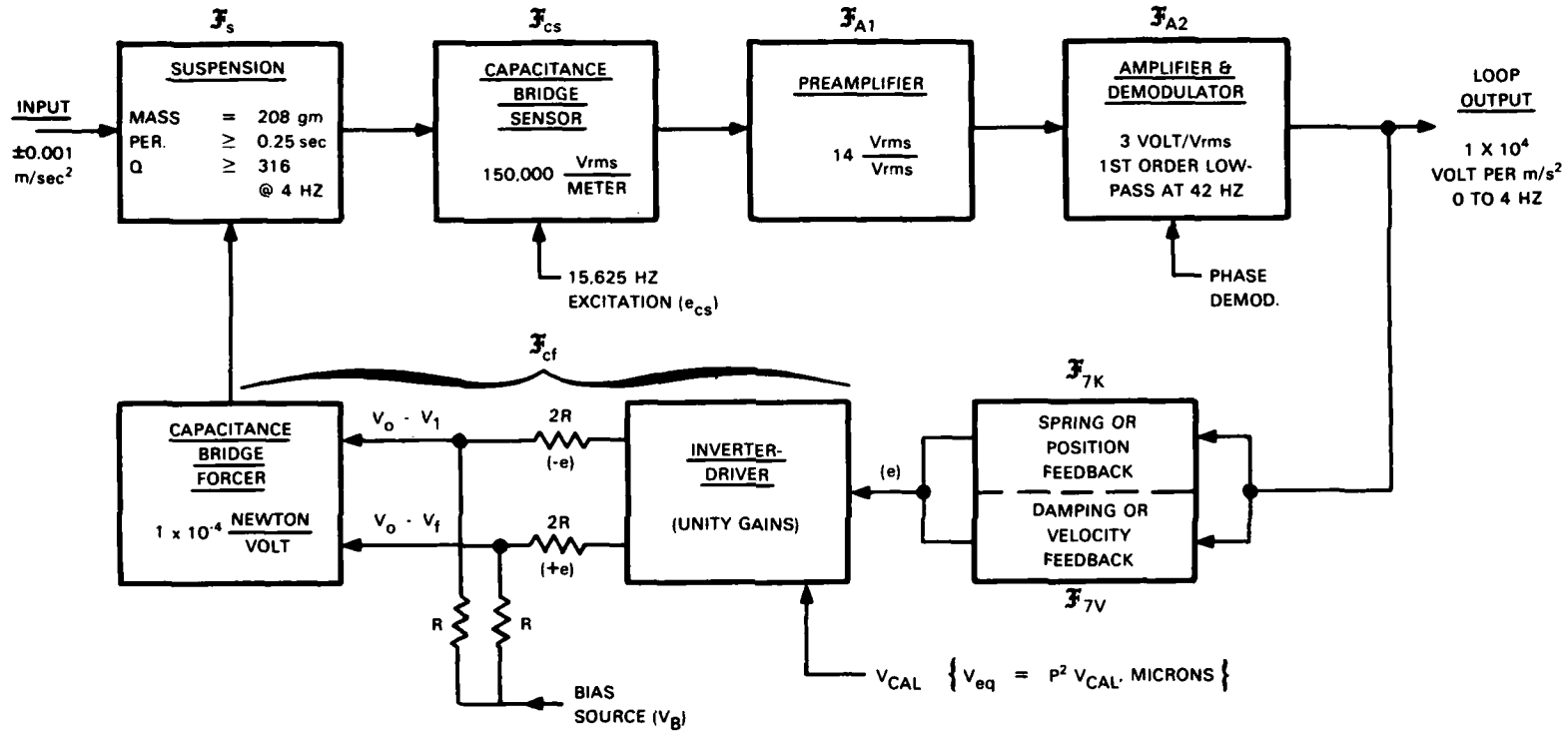

EXCITATION AMPLITUDE (e_{cs}) SET FOR INDIVIDUAL UNITS
$e_{cs} = S_o$ (56250) Vrms
Where S_o = PLATE SPACING IN METERS, (8.8t x 10^{-5}m, nom.)
TO GIVE 150,000 Vrms/METER.

BIAS VOLTAGE (V_B) SET FOR INDIVIDUAL UNITS TO GIVE 1 x 10^{-4} NEWTON/VOLT.
FINAL PLATE BIAS IS 21 TO 36 Vdc, TYPICAL.

POSITION FEEDBACK ($\mathcal{F}_{7K}$) SET FOR INDIVIDUAL UNITS TO GIVE 4 HZ CORNER.
VELOCITY FEEDBACK ($\mathcal{F}_{7V}$) SET FOR INDIVIDUAL UNITS FOR 0.7 DAMPING AT 4 HZ.

FIGURE 1-1. LOOP CONFIGURATION FOR 44000

G 12664A

The components $\mathcal{F}_{7K}$ and $\mathcal{F}_{7V}$ become equal in magnitude in the 2 to 3 Hz range, and, consequently, the linearity condition cannot be approximated in the short-period data band. Therefore, nonlinearity continued to be a major issue after April 1980 since short-period performance was in question. Nonlinearity in the short-period can also degrade long-period performance by generating intermodulation distortion products.

Major theoretical and experimental effort was directed at the short-period nonlinearity issue. Theoretical results predicted short-period linearity to be better than 0.1% and that distortion products with a high cultural background would be less than the specified long-period noise level.

Comparative borehole testing in Garland during March 1982 using the 44000 engineering model and a 36000 seismometer demonstrated that the linearity methods were successful.

During the same test series in March 1982, it was verified that the short-period response was not uniform from channel-to-channel and differed from the theoretical response. These response errors were judged to be due to errors in determining the transducer plate spacing, s_o. Since sensing and forcing loop parameters are computed using the plate spacing, it must be accurately determined.

To ensure that the plate spacing could be accurately measured and loop parameters set correctly, the following actions were taken.

a. Bridge excitation level was selected for individual units to maintain a uniform capacitance bridge sensitivity of 150,000 volts/meter.

b. The bias voltage source was increased from 60 Vdc to 80 Vdc to extend the bias voltage selection range.

c. A comprehensive Sensor Test and Calibration Procedure and test fixtures were developed to utilize the precision leveling/positioning mechanisms to set up and calibrate the total sensor channel.

The improved calibration procedure revealed that the response characteristics observed in March 1982 were not due to inaccuracy in determining plate spacing. The transfer function used for the electrostatic forcing transducer does not hold in the corner frequency range.

Using the improved calibration procedure and fixtures, it was possible to set the corner frequency to the specified 4 Hz corner frequency. The loop parameters actually required differed drastically with those computed on the basis of plate spacing.

The method used to estimate short-period linearity could not be applied for empirically determined loop parameters. Although the statistical confidence of surface bench measurements was low, nonlinearities on the order of 1% were suspected. If such nonlinearities were involved, then it would be a grave error to empirically set the corner frequency to 4 Hz. The balance of this paper discusses the methods used to resolve the response-nonlinearity question.

The results show that required linearity and a 4 Hz corner frequency cannot be achieved. It is on this basis that we have recommended that present systems, with loop parameters set by the method for which linearity has been demonstrated, be restricted to long-period measurements. To achieve a broad-band response, we must abandon the electrostatic feedback transducer.

2. INERTIAL SEISMOMETER CHARACTERIZATION

The seismometer to be considered here consists of a two-body mechanical oscillator constrained to a single degree of freedom and an electrostatic transducer which is sensitive to the relative position of the two bodies. One body, of mass M_a, is referred to as the frame or support. The second body of mass, M_b, is referred to as the suspended or inertial mass or the bob. Measuring along the axis of motion with respect to inertial rest positions and denoting the inertial coordinate of the support (M_a) by "$\bar{y}$", and the inertial coordinate of the bob (M_b) by "$\bar{x}$", the equations of motion are

$$\ddot{\bar{x}} + \dot{\bar{x}}\left(\frac{r}{M_b}\right) + \bar{x}\left(\frac{K}{M_b}\right) = \frac{X'}{M_b} + \dot{\bar{y}}\left(\frac{r}{M_b}\right) + \bar{y}\left(\frac{K}{M_b}\right) \qquad (2\text{-}1)$$

$$\ddot{\bar{y}} + \dot{\bar{y}}\left(\frac{r}{M_a}\right) + \bar{y}\left(\frac{K}{M_a}\right) = \frac{Y'}{M_a} + \dot{\bar{x}}\left(\frac{r}{M_a}\right) + \bar{x}\left(\frac{K}{M_a}\right) \qquad (2\text{-}2)$$

and the relative motion is given by the difference of (2-1) and (2-2), e.g.,

$$\ddot{x} + \dot{x}\left(\frac{r}{M_o}\right) + x\left(\frac{K}{M_o}\right) + \left(\frac{X'}{M_b} - \frac{Y'}{M_a}\right) \qquad (2\text{-}3)$$

where: $x = \bar{x} - \bar{y}$ is the coordinate of the bob relative to the frame;

$M_o = \dfrac{M_a M_b}{M_a + M_b}$ is the reduced mass of the two body system;

$\left(\dfrac{X'}{M_b} - \dfrac{Y'}{M_a}\right)$ is the force field acting on the mass M_b relative to the mass M_a;

X', Y' are forces exerted directly on M_b or M_a respectively;

K is the rate of change of the restoring force with relative displacement;

r is the coefficient of the viscous damping force due to losses within the mechanical system tending to reduce the relative velocity.

$$(\dot{}),\ (\ddot{}) \ = \ d(\ )/dt,\ \ d^2(\ )/dt^2$$

In many applications, the frame M_a can be considered rigidly connected to a mass M_c much larger than M_b, whereby

$$\lim_{M_c \to \infty} M_o \ = \ \lim_{M_c \to \infty} \frac{M_b\,(M_a + M_c)}{M_b + (M_a + M_c)} \ = \ M_b \ = \ M \qquad (2\text{-}4)$$

and the relative motion is given by

$$\ddot{x}M \ + \ \dot{x}r \ + \ xK \ = \ X' - \ddot{y}M \qquad (2\text{-}5)$$

where $y = \bar{y}$.

2.1 SUSPENSION-TRANSDUCER CHARACTERIZATION

Figure 2-1 indicates the components, constants, and variables involved in the suspension-transducer interfaces. Symbols and functions are described as follows.

Symbol	Function/Description
$\bar{y}$	Inertial coordinate of suspension frame, meters.
$\bar{x}$	Inertial coordinate of suspension bob, meters.
M	Mass of suspension bob, kilograms (kg).
C_{ax}	Position-dependent capacitance of left frame plate to the grounded bob, farads.
C_{bx}	Position-dependent capacitance of right frame plate to the grounded bob, farads.
C_a	Fixed excitation coupling capacitor to left plate, farads.
C_b	Fixed excitation coupling capacitor to right plate, farads.
e_a	Loop feedback voltage for left plate, volts
e_b	Loop feedback for right plate, volts
V_b	Bias source voltage, volts

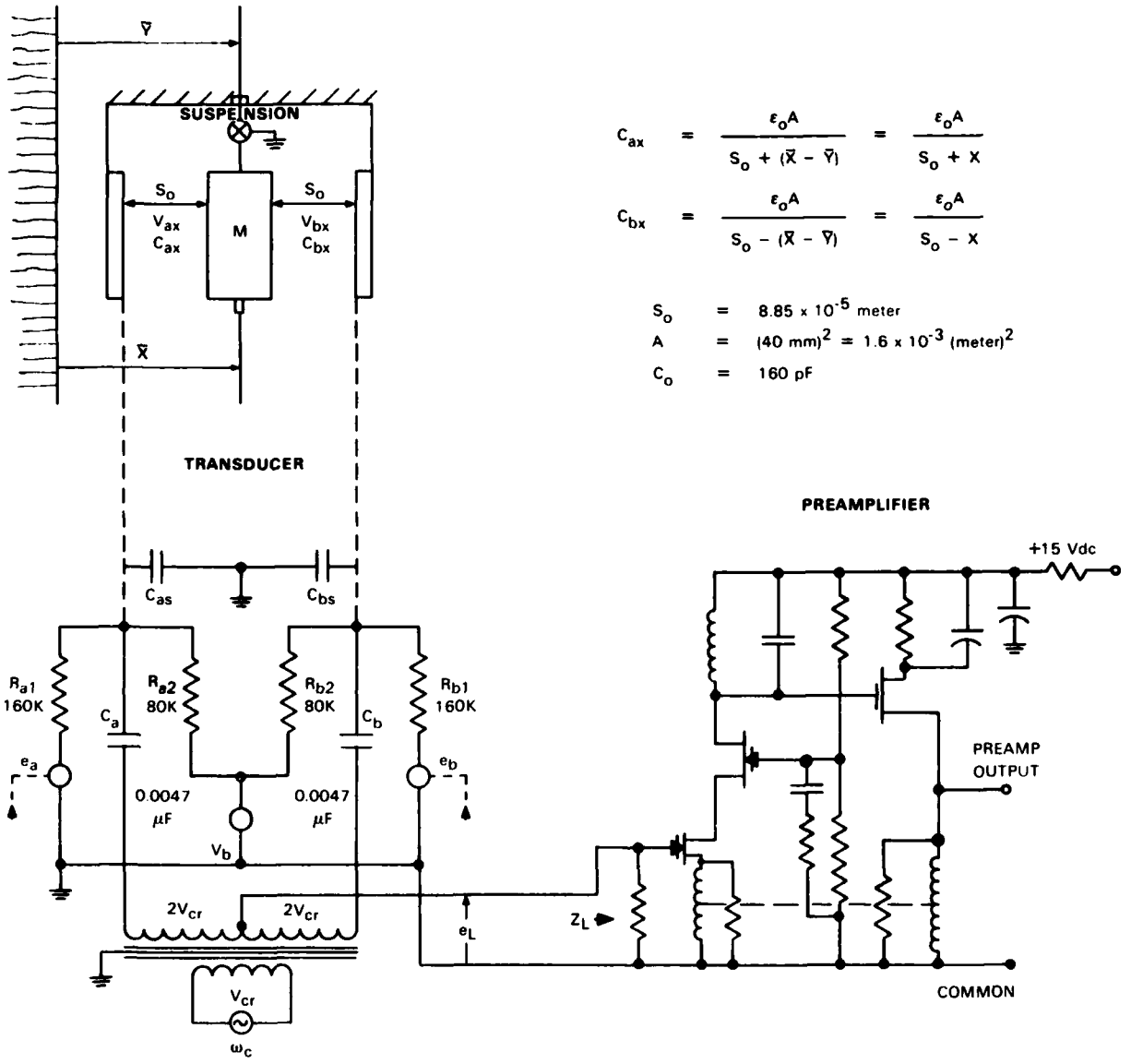

$$C_{ax} = \frac{\varepsilon_o A}{S_o + (\bar{X} - \bar{Y})} = \frac{\varepsilon_o A}{S_o + X}$$

$$C_{bx} = \frac{\varepsilon_o A}{S_o - (\bar{X} - \bar{Y})} = \frac{\varepsilon_o A}{S_o - X}$$

S_o = 8.85×10^{-5} meter

A = $(40\ mm)^2 = 1.6 \times 10^{-3}\ (meter)^2$

C_o = 160 pF

$$\frac{1}{Z_A} = j\omega_c C_{ax} + \frac{1}{R_{a1}} + \frac{1}{R_{a2}} + j\omega_c C_{as} \quad ; \quad \frac{1}{Z_C} = j\omega_c C_a$$

$$\frac{1}{Z_B} = j\omega_c C_{bx} + \frac{1}{R_{b1}} + \frac{1}{R_{b2}} + j\omega_c C_{bs} \quad ; \quad \frac{1}{Z_D} = j\omega_c C_b$$

FIGURE 2-1. SUSPENSION - TRANSDUCER INTERFACES

G15140

R_{a1}, R_{a2}	Summing/weighting resistors for feedback voltage and bias voltage for the left plate, ohms.
R_{b1}, R_{b2}	Summing/weighting resistors for feedback voltage and bias voltage for the right plate, ohms.
V_{cr}	Carrier source excitation, 15625 Hz, (~5), Vrms.
Z_L	Input impedance of the preamplifier
e_L	Capacitance bridge amplitude modulated output to preamplifier, Vrms.
V_{ax}	The instantaneous potential of the left frame plate with respect to the grounded bob, volts.
V_{bx}	The instantaneous potential of the right frame plate with respect to the grounded bob, volts.
Z_A	Impedance of left plate to common at carrier frequency ω_c.
Z_B	Impedance of right plate to common at carrier frequency ω_c.
Z_C	Impedance of C_a at carrier frequency ω_c.
Z_D	Impedance of C_b at carrier frequency ω_c.
ϵ_o	Permittivity of space, 8.85×10^{-12} farad per meter.

Equation 2-5 relates suspension parameters and differential bob-frame motion to the earth input, yM, and the force term X'. The term X' is comprised of the several force components developed by the electrostatic forcing transducer.

The principal electrostatic force is that discussed by Monroe and is expressed here as

$$\mathcal{F}_p = \frac{-\epsilon_o A\, V_{ax}\, V_{ax}^*}{2\,(s_o + x)^2} + \frac{\epsilon_o A\, V_{bx}\, V_{bx}^*}{2\,(s_o - x)^2} \qquad (2.1\text{-}1)$$

where: A is effective area of the bob-frame capacitance, m^2. Since V_{ax} and V_{bx} are complex functions, conjugate functions V_{ax}^* and V_{bx}^* are used. Note that $\mathcal{F}_p$ is position dependent. The capacitance bridge sensor produces a signal which is dependent on the bob position relative to the frame. This signal and its derivatives are components of V_{ax} and V_{bx}. Independent of these signals, $\mathcal{F}_p$ depends on the position of the bob relative to the frame.

A velocity-dependent force can also be identified. This component is associated with the work done in mechanically moving the plates of a charged capacitor. When the relative position is changing, charge redistribution produces current in the electrical circuits and dissipation in electrical resistances. An exact expession for the velocity-dependent force is difficult; however, a worst-case approximation for the mechanical viscous force coefficient, r_e, will suffice.

$$\mathcal{F}_v = -\dot{x}r_e;\ r_e \doteq (\epsilon_o A)^2 \left[\frac{V_{ax}\, V_{ax}^*\, R_{a12}}{(s_o + x)^4} + \frac{V_{bx}\, V_{bx}^*\, R_{b12}}{(s_o - x)^4}\right] \quad (2.1\text{-}2)$$

where $R_{a12} = \dfrac{R_{a1}\, R_{a2}}{R_{a1} + R_{a2}}$; $R_{b12} = \dfrac{R_{b1}\, R_{b2}}{R_{b1} + R_{b2}}$

The suspension-forcing transducer interface can be summaized with the following expression.

$$\ddot{x}M + \dot{x}r_m + xK_m = -\ddot{y}M + \frac{\epsilon_o A}{2}\left[\frac{-V_{ax}\, V_{ax}^*}{(s_o + x)^2} + \frac{V_{bx}\, V_{bx}^*}{(s_o - x)^2}\right] \quad (2.1\text{-}3)$$

$$-\dot{x}\,(\epsilon_o A)^2 \left[\frac{V_{ax}\, V_{ax}^*\, R_{a12}}{(s_o + x)^4} + \frac{V_{bx}\, V_{bx}^*\, R_{b12}}{(s_o - x)^4}\right]$$

where: r_m is coefficient damping due to the mechanical system, Newton per meter/sec; and K_m is coefficient of restoring force due to the mechanical system, Newton per meter.

The suspension-sensing transducer interface can be described as follows. The term ^{P}ct indicates an amplitude-modulated carrier signal. The capacitance bridge sensor output signal, e_L, developed across the amplifier input impedance, Z_L, can be written as

$$e_L = \frac{\left|(2V_{cr})\, Z_L(Z_C + Z_A) - (2V_{cr})(Z_L)(Z_B + Z_D)\right| \epsilon^{P}ct}{Z_L(Z_C + Z_A) + Z_L(Z_B + Z_D) + (Z_C + Z_A)(Z_B + Z_D)} \quad (2.1\text{-}4)$$

or, with some manipulation,

$$e_L = \frac{(2V_{cr})\ (Z_C - Z_D + Z_A - Z_B)\ \epsilon^{P}ct}{Z_A + Z_B + Z_C + Z_D + \dfrac{1}{Z_L}(Z_C + Z_A)(Z_B + Z_D)}$$

Using the cascode FET input stage allows Z_L to be made very large - typically 10pF and 400 Mohm. This allows 2.1-4 to be approximated by

$$e_L = \frac{(2V_{cr})\ (Z_C - Z_D + Z_A - Z_B)}{Z_A + Z_B + Z_C + Z_D}\epsilon^{Pct} = (2V_{cr})\frac{\Delta Z}{Z_T} \qquad (2.1\text{-}5)$$

where $\Delta Z = Z_C - Z_D + Z_A - Z_B$ and $Z_T = Z_A + Z_B + Z_C + Z_D$ (2.1-6)

Note that the impedances Z_A and Z_B, and, consequently, ΔZ and Z_T are functions of x.

Now, the expressions for the feedback voltages e_a and e_b can be written.

$$\left.\begin{aligned} &e_a = e_L \mathcal{F}_{A1}\mathcal{F}_{A2}(\mathcal{F}_{7K} + \mathcal{F}_{7V})\epsilon^{-Pct}; \quad e_b = -e_L\mathcal{F}_{A1}\mathcal{F}_{A2}(\mathcal{F}_{7K} + \mathcal{F}_{7V})\epsilon^{-Pct} \\ &\text{or setting } \mathcal{F}_K = \mathcal{F}_{A1}\mathcal{F}_{A2}\mathcal{F}_{7K} \text{ and } \mathcal{F}_V = \mathcal{F}_{A1}\mathcal{F}_{A2}\mathcal{F}_{7V} \\ &\text{then} \quad e_a = e_L(\mathcal{F}_K + \mathcal{F}_V)\epsilon^{-Pct}; \quad e_b = -e_L(\mathcal{F}_K + \mathcal{F}_V)\epsilon^{-Pct} \end{aligned}\right\} (2.1\text{-}7)$$

Note that the transfer functions $\mathcal{F}_K$ and $\mathcal{F}_V$ contain a demodulation term, ϵ^{-Pct}, for the modulated signal e_L.

In addition to the bias voltage and the feedback voltage, the voltages V_{ax} and V_{bx} have a third component due to the carrier excitation. The voltage e_{AC} for the left plate and the voltage e_{BC} for the right plate are as follows.

$$e_{AC} = Z_A \left[\frac{2V_{cr}(Z_L + Z_B + Z_D) + 2V_{cr}Z_L}{(Z_C + Z_A)(Z_L + Z_B + Z_D) + Z_L(Z_B + Z_D)}\right] \epsilon^{P_{ct}}$$

$$e_{BC} = -Z_B \left[\frac{2V_{cr}(Z_L + Z_C + Z_A) + 2V_{cr}Z_L}{(Z_B + Z_D)(Z_L + Z_C + Z_A) + Z_L(Z_C + Z_A)}\right] \epsilon^{P_{ct}} \quad (2.1\text{-}8)$$

and rearranging

$$e_{AC} = \frac{2V_{cr}\left[1 + \dfrac{1}{1 + (Z_B + Z_D)(1/Z_L)}\right]\epsilon^{P_{ct}}}{1 + Z_C/Z_A + \dfrac{(Z_B + Z_D)(1/Z_A)}{1 + (Z_B + Z_D)(1/Z_L)}}$$

$$e_{BC} = \frac{-2V_{cr}\left[1 + \dfrac{1}{1 + (Z_A + Z_C)(1/Z_L)}\right]\epsilon^{P_{ct}}}{1 + Z_D/Z_B + \dfrac{(Z_C + Z_A)(1/Z_B)}{1 + (Z_C + Z_A)(1/Z_L)}}$$

Again, since $Z_L >> (Z_B + Z_D)$, $Z_L >> (Z_A + Z_C)$ the expressions can be approximated as follows.

$$e_{AC} = 2V_{cr}\epsilon^{P_{ct}}\left[\frac{2Z_A}{Z_A + Z_B + Z_C + Z_D}\right] = 2\,V_{cr}\epsilon^{P_{ct}}\left(\frac{2Z_A}{Z_T}\right)$$

$$e_{BC} = -2V_{cr}\epsilon^{P_{ct}}\left[\frac{2Z_B}{Z_A + Z_B + Z_C + Z_D}\right] = -2V_{cr}\epsilon^{P_{ct}}\left(\frac{2Z_B}{Z_T}\right) \quad (2.1\text{-}9)$$

Finally, the voltages V_{ax} and V_{bx} can be expressed as follows.

$$V_{ax} = e_a\left(\frac{R_{a2}}{R_{a1} + R_{a2}}\right) + V_B\left(\frac{R_{a1}}{R_{a1} + R_{a2}}\right) + e_{AC} \;;$$

$$V_{ax} = e_L\left(\frac{R_{a2}}{R_a}\right)(\mathcal{F}_K + \mathcal{F}_V)\epsilon^{-P_{ct}} + V_B\left(\frac{R_{a1}}{R_a}\right) + 2\,V_{cr}\epsilon^{P_{ct}}\left(\frac{2Z_A}{Z_T}\right);$$

$$V_{ax} = 2V_{cr}\left(\frac{\Delta Z}{Z_T}\right)\left(\frac{R_{a2}}{R_a}\right)(\mathcal{F}_K + \mathcal{F}_V) + V_B\left(\frac{R_{a1}}{R_a}\right) + 2V_{cr}\epsilon^{P_{ct}}\left(\frac{2Z_A}{Z_T}\right). \quad (2.1\text{-}10)$$

Similarly,

$$V_{bx} = e_b \left(\frac{R_{b2}}{R_{b1} + R_{b2}}\right) + V_B \left(\frac{R_{b1}}{R_{b1} + R_{b2}}\right) + e_{BC} \ ;$$

$$V_{bx} = -e_L \left(\frac{R_{b2}}{R_b}\right) (\mathcal{F}_K + \mathcal{F}_V)\epsilon^{-P_{ct}} + V_B \left(\frac{R_{b1}}{R_b}\right) - 2 V_{cr} P_{ct} \left(\frac{2Z_B}{Z_T}\right) ;$$

$$V_{bx} = -2V_{cr} \left(\frac{\Delta Z}{Z_T}\right)\left(\frac{R_{b2}}{R_b}\right) (\mathcal{F}_K + \mathcal{F}_V) + V_B \left(\frac{R_{b1}}{R_b}\right) - 2V_{cr}\epsilon^{P_{ct}} \left(\frac{2Z_B}{Z_T}\right) . \quad (2.1\text{-}11)$$

where $R_{a1} + R_{a2} = R_a$ and $R_{b1} + R_{b2} = R_b$.

Equations 2.1-10 and 2.1-11, and their complex conjugates, will be used in the following sections to expand the basic equation of motion in 2.1-3.

3. DISCUSSION OF TERMS

The plate potentials V_{ax} and V_{bx} include: a) the dc component due to the dc bias voltage; b) data frequency components of amplitude modulated carrier and feedback signals; and c) carrier frequency components. It is necessary to identify terms and treat them with respect to the frequency range in which they interact with the suspension.

Figure 3 shows the expansion of terms for $V_{ax}V_{ax}^*$ and $V_{bx}V_{bx}^*$. The product of the function with its complex conjugate gives the square of the absolute value of the function which is needed for the analysis of electrostatic forces.

3.1 CARRIER FREQUENCY EXCITATION

Carrier operators have been indicated by ϵ^{Pct} and ϵ^{-Pct}. In figure 3, terms 3a-9 and 3b-9 contain both operators and will result in force components which vary with $Z_AZ_A^*$ and $Z_BZ_B^*$, respectively.

Terms 3a-5, 3a-6, 3a-7, 3a-8 and 3b-5, 3b-6, 3b-7, 3b-8 containing only ϵ^{Pct} or ϵ^{-Pct} singly vary at the carrier frequency. Since the highest data frequency is much less than the carrier frequency, the mean value of these terms in the band of interest can be taken as zero.

3.2 IMPEDANCE FACTORS

The impedances of ΔZ, Z_T and the components therein represent impedances at the carrier frequency which are modified by the bob-frame position. These transducer impedances have time constants corresponding to about 700 Hz and have not been included in the data band transfer functions presented here.

When factor $\Delta Z\ Z^*/Z_TZ_T^*$ is expanded in its position-dependent terms, the numerator vanishes.

$$\left.\begin{aligned} \text{NUMERATOR} &= \frac{C_{ax}^2 - 2\,C_{ax}\,C_{bx} + C_{bx}^2}{\text{DENOMINATOR}} \\ &= \frac{(\epsilon_oA)^2\left[\dfrac{(s_o - X)^2 - 2(s_o + X)(s_o - X) + (s_o + X)^2}{(s_o + X)^2\,(s_o - X)^2}\right]}{\text{DENOMINATOR}} = 0 \end{aligned}\right\} (3.2\text{-}1)$$

This restates that the resultant force in a symmetrical transducer is zero in the absence of a bias component.

$$V_a V_a^* Z_T Z_T^* = \Delta Z \Delta Z^* \left[\left(2V_{cr} \frac{R_{a2}}{R_a} \right)^2 \left(\mathcal{F}_K \mathcal{F}_K^* + \mathcal{F}_V \mathcal{F}_V^* + \mathcal{F}_K \mathcal{F}_V^* + \mathcal{F}_K^* \mathcal{F}_V \right) \right] \quad 3a\text{-}1$$

$$+ \; Z_T Z_T^* \left[\left(V_B \frac{R_{a1}}{R_a} \right)^2 \right] \quad 3a\text{-}2$$

$$+ \; \Delta Z Z_T^* \left[2V_{cr} \, V_B \frac{R_{a1}}{R_a} \frac{R_{a2}}{R_a} \left(\mathcal{F}_K + \mathcal{F}_V \right) \right] \quad 3a\text{-}3$$

$$+ \; \Delta Z^* Z_T \left[2V_{cr} V_B \frac{R_{a1}}{R_a} \frac{R_{a2}}{R_a} \left(\mathcal{F}_K^* + \mathcal{F}_V^* \right) \right] \quad 3a\text{-}4$$

$$+ 2\Delta Z Z_A^* \left[(2V_{cr})^2 \frac{R_{a2}}{R_a} \epsilon^{-P_{ct}} \left(\mathcal{F}_K + \mathcal{F}_V \right) \right] \quad 3a\text{-}5$$

$$+ 2\Delta Z^* Z_A \left[(2V_{cr})^2 \frac{R_{a2}}{R_a} \epsilon^{P_{ct}} \left(\mathcal{F}_K^* + \mathcal{F}_V^* \right) \right] \quad 3a\text{-}6$$

$$+ \; 2Z_T Z_A^* \left[2V_{cr} \, V_B \frac{R_{a1}}{R_a} \epsilon^{-P_{ct}} \right] \quad 3a\text{-}7$$

$$+ \; 2Z_T^* Z_A \left[2V_{cr} \, V_B \frac{R_{a1}}{R_a} \epsilon^{P_{ct}} \right] \quad 3a\text{-}8$$

$$+ \; 4Z_A Z_A^* \left[(2V_{cr})^2 \epsilon^{P_{ct}} \epsilon^{-P_{ct}} \right] \quad 3a\text{-}9$$

FIGURE 3. EXPANSION OF $V_{ax}V_{ax}$ AND $V_{bx}V_{bx}$ (SHEET 1 OF 2)

$$V_b V_b^* \; Z_T Z_T^* = \Delta Z \Delta Z^* \left[\left(2V_{cr} \frac{R_{b2}}{R_b} \right)^2 \left(\mathcal{F}_K \mathcal{F}_K^* + \mathcal{F}_V \mathcal{F}_V^* + \mathcal{F}_K \mathcal{F}_V^* + \mathcal{F}_K^* \mathcal{F}_V \right) \right] \quad 3b\text{-}1$$

$$+ \; Z_T Z_T^* \left[\left(V_B \frac{R_{b1}}{R_b} \right)^2 \right] \quad 3b\text{-}2$$

$$- \; \Delta Z Z_T^* \left[2V_{cr} \; V_B \frac{R_{b1}}{R_b} \; \frac{R_{b2}}{R_b} \; (\mathcal{F}_K + \mathcal{F}_V) \right] \quad 3b\text{-}3$$

$$- \; \Delta Z^* Z_T \left[2V_{cr} V_B \; \frac{R_{b1}}{R_b} \; \frac{R_{b2}}{R_b} \; (\mathcal{F}_K^* + \mathcal{F}_V^*) \right] \quad 3b\text{-}4$$

$$+2 \Delta Z Z_B^* \left[(2V_{cr})^2 \frac{R_{b2}}{R_b} \epsilon^{-P_{ct}} \; (\mathcal{F}_K + \mathcal{F}_V) \right] \quad 3b\text{-}5$$

$$+2 \Delta Z^* Z_B \left[(2V_{cr})^2 \; \frac{R_{b2}}{R_b} \; \epsilon^{P_{ct}} \; (\mathcal{F}_K^* + \mathcal{F}_V^*) \right] \quad 3b\text{-}6$$

$$- \; 2 Z_T Z_B^* \left[2V_{cr} \; V_B \; \frac{R_{b1}}{R_b} \; \epsilon^{-P_{ct}} \right] \quad 3b\text{-}7$$

$$- \; 2 Z_T^* Z_B \left[2V_{cr} \; V_B \; \frac{R_{b1}}{R_b} \; \epsilon^{P_{ct}} \right] \quad 3b\text{-}8$$

$$+ \; 4 Z_B Z_B^* \left[(2V_{cr})^2 \; \epsilon^{P_{ct}} \epsilon^{-P_{ct}} \right] \quad 3b\text{-}9$$

FIGURE 3. EXPANSION OF $V_{ax}V_{ax}$ AND $V_{bx}V_{bx}$ (SHEET 2 OF 2)

In the later expressions, the bridge is assumed to be perfectly symmetrical, i.e.,

$$\left.\begin{aligned} &R_{a1} = R_{b1} \equiv R_1 \;;\; R_{a2} = R_{b2} \equiv R_2 \;;\; R_{a1} + R_{a2} = R_{b1} + R_{b2} \equiv R; \\ &\frac{R_{a1} + R_{a2}}{R_{a1}R_{a2}} = \frac{R_{b1} + R_{b2}}{R_{b1}R_{b2}} \equiv R12 = \frac{1}{g12} \\ &C_{as} = C_{bs} = C_s \end{aligned}\right\} \quad (3.2\text{-}2)$$

The equation of motion from 2.1-3 can be written using the impedance notations as shown in 3.2-3.

$$\ddot{x}M + \dot{x}r_m + xK_m = \ddot{y}M + \left(\frac{\epsilon_o A}{2}\right)\left(V_B \frac{R_1}{R}\right)^2 \left[\frac{1}{(s_o - x)^2} - \frac{1}{(s_o + x)^2}\right] +$$

$$- \left(\frac{\epsilon_o A}{2}\right)\left(2V_{cr}\, V_B \frac{R_1}{R}\, \frac{R_2}{R}\right)\left[\frac{\Delta Z Z_T^* (\mathcal{F}_K + \mathcal{F}_V) + \Delta Z^* Z_T (\mathcal{F}_K^* + \mathcal{F}_V^*)}{Z_T Z_T^*}\right]\left[\frac{1}{(s_o - x)^2} + \frac{1}{(s_o + x)^2}\right] +$$

$$+ \left(\frac{\epsilon_o A}{2}\right)(4)(2V_{cr})^2 \frac{\left[\frac{Z_B Z_B^*}{(s_o - x)^2} - \frac{Z_A Z_A^*}{(s_o + x)^2}\right]}{Z_T Z_T^*} +$$

$$- \dot{x}(\epsilon_o A)^2 R_{12}\left(2V_{cr} V_B \frac{R_1}{R}\, \frac{R_2}{R}\right)\left[\frac{\Delta Z Z_T^* (\mathcal{F}_K + \mathcal{F}_V) + \Delta Z^* Z_T (\mathcal{F}_K^* + \mathcal{F}_V^*)}{Z_T Z_T^*}\right]\left(\frac{1}{(s_o+x)^4} - \frac{1}{(s_o-x)^4}\right)$$

$$- \dot{x}(\epsilon_o A)^2 R_{12}\left(V_B \frac{R_1}{R}\right)^2 \left[\frac{1}{(s_o + x)^4} + \frac{1}{(s_o - x)^4}\right] +$$

$$- \dot{x}(\epsilon_o A)^2 R_{12}(4)(2V_{cr})^2 \frac{\left[\frac{Z_A Z_A^*}{(s_o + x)^4} + \frac{Z_B Z_B^*}{(s_o - x)^4}\right]}{Z_T Z_T^*} . \quad (3.2\text{-}3)$$

4. EXPLICIT POSITION TERMS

The impedance terms have allowed intermediate expressions to be written and manipulated in abbreviated form. Ultimately, the impedances must be written as explicit functions of bob-frame position to complete the equation of motion in the variable x. The result is given in figure 4.

The symbols are as previously defined with two exceptions. The capacitance C_{ab} is the series value of C_a and C_b.

$$C_{ab} = \frac{C_a C_b}{C_a + C_b} \qquad 4\text{-}1$$

The components of the loop transfer function $\mathcal{F}_K$ and $\mathcal{F}_V$ are complex functions of frequency having real (R_e) and imaginary (I_m) parts. Therefore,

$$\left.\begin{aligned} \mathcal{F}_K &= R_e\mathcal{F}_K + jI_m\mathcal{F}_K \;;\; \mathcal{F}_K^* = R_e\mathcal{F}_K - jI_m\mathcal{F}_K \\ \mathcal{F}_V &= R_e\mathcal{F}_V + jI_m\mathcal{F}_V \;;\; \mathcal{F}_V^* = R_e\mathcal{F}_V - jI_m\mathcal{F}_V \end{aligned}\right\} \qquad 4\text{-}2$$

In the data band, the principal part of $\mathcal{F}_K$ is $R_e\mathcal{F}_K$, and the principal part of $\mathcal{F}_V$ is $I_m\mathcal{F}_V$.

The form of the equation is similar to that of 3.2-3 to reveal the transition from impedance functions to position terms. The equation can be reduced, expanded, approximated, and otherwise manipulated indefinitely. We have yet to find a form that suggests an analytic solution. An analytic solution would allow coefficients to be optimized for response and linearity. Conversely, a numerical solution with assumed coefficients can describe resulting responses and linearities which could possibly converge to an optimum configuration.

4.1 RECOMMENDATIONS

Experience dims the prospects of a solution which provides the response, linearity and predictability desired here. This suggests that the most useful benefit of the electrostatic transducer development is the performance achieved in the long-period band where the Monroe Linearity Condition can be approximated.

Current applications for a borehole seismometer system require an extension, rather than a reduction, in data bandwidth. The electromagnetic feedback transducer will provide improved linearity and allow data bandwidth to be extended. The Model 44000 seismometers can be converted from electrostatic to electromagnetic feedback transducer, and we recommend this course of action.

$$\frac{1}{(s_o + x)^4} + \frac{1}{(s_o - x)^4}\Bigg|$$

$$\left(1 + \frac{C_s}{C_{ab}}\right) + (\epsilon_o A)^2 \left(\frac{1}{(s_o - x)^2} - \frac{1}{(s_o + x)^2}\right) + \left(2C_s + \frac{C_s^2}{C_{ab}} + \frac{g_{12}^2}{\omega_c^2 C_{ab}}\right)(\epsilon_o A)\left(\frac{1}{(s_o - x)} - \frac{1}{(s_o + x)}\right)\Bigg\}\left[\frac{1}{(s_o + x)^4} - \frac{1}{(s_o - x)^4}\right]$$

$$\frac{g_{12} C_s}{\omega_c C_{ab}}\right)(\epsilon_o A)\left(\frac{1}{(s_o - x)} - \frac{1}{s_o + x}\right)\Bigg|$$

$$\frac{1}{(s_o + x)^2}\left[(\epsilon_o A)^2\left(\frac{1}{(s_o - x)^2}\right) + 2C_s(\epsilon_o A)\left(\frac{1}{(s_o - x)}\right) + \frac{g_{12}^2}{\omega_c^2} + C_s^2\right]$$

$$x)^2}\right) + \left(1 + \frac{C_s}{C_{ab}}\right) + (\epsilon_o A)^2\left(\frac{1}{(s_o + x)^2} - \frac{1}{(s_o + x)^2}\right) + \left(2C_s + \frac{C_s^2}{C_{ab}} + \frac{g_{12}^2}{\omega_c^2 C_{ab}}\right)(\epsilon_o A)\left(\frac{1}{(s_o - x)} - \frac{1}{(s_o + x)}\right)\Bigg\}\left[\frac{1}{(s_o + x)^4} - \frac{1}{(s_o - x)^4}\right]$$

$$\frac{g_{12}}{\omega_c} + \frac{2g_{12} C_s}{\omega_c C_{ab}}\right)(\epsilon_o A)\left(\frac{1}{s_o - x} - \frac{1}{s_o + x}\right)$$

$$^2\Bigg| + \frac{1}{(s_o - x)^4}\left[(\epsilon_o A)^2\left(\frac{1}{(s_o + x)^2}\right) + 2C_s(\epsilon_o A)\left(\frac{1}{s_o - x}\right) + \frac{g_{12}^2}{\omega_c^2} + C_s^2\right]\Bigg\}$$

$$\frac{1}{+ x)^2 (s_o - x)}\Bigg| + \left(\frac{g_{12}^2}{\omega_c^2 C_{ab}^2} + \frac{C_s^2}{C_{ab}^2} + \frac{2C_s}{C_{ab}} + 1\right)(\epsilon_o A)^2\left|\frac{1}{(s_o - x)^2} + \frac{1}{(s_o + x)^2}\right| + \left(\frac{8C_s}{C_{ab}} + \frac{4C_s^2}{C_{ab}^2} + 2\right)(\epsilon_o A)^2\left|\frac{1}{(s_o - x)(s_o + x)}\right| .$$

$$\frac{1}{(s_o + x)}\Bigg| + 4C_s^2 + \frac{4g_{12}^2}{\omega_c^2} .$$

FIGURE 4. EQUATION OF MOTION, SUSPENSION AND ELECTROSTATIC TRANSDUCER

$$\ddot{x}M + x\dot{r}_m + xK_m = -yM + \left(\frac{\epsilon_o A}{2}\right)\left(V_B \frac{R_1}{R}\right)^2 \left[\frac{1}{(s_o - x)^2} - \frac{1}{(s_o + x)^2}\right] - \dot{x}(\epsilon_o A)^2 R_{12} \left(V_B \frac{R_1}{R}\right)^2 \left[\frac{1}{(s_o + x)^4} +\right.$$

$$- \left(\frac{\epsilon_o A}{2}\right)\left(2V_{cr}V_B \frac{R_1}{R} \frac{R_2}{R}\right)\left\{\begin{array}{l} 2(R_e\mathfrak{F}_K + R_e\mathfrak{F}_V)\left[\frac{(\epsilon_o A)^3}{C_{ab}}\left(\frac{1}{(s_o - x)^2 (s_o + x)} - \frac{1}{(s_o - x)(s_o + x)^2}\right) + \left(1 + \frac{C_s}{C_{ab}}\right.\right. \\ - 2(I_m\mathfrak{F}_K + I_m\mathfrak{F}_V)\left[\left(\frac{g_{12}}{\omega_C C_{ab}}\right)(\epsilon_o A)^2\left(\frac{1}{(s_o - x)^2} - \frac{1}{(s_o + x)^2}\right) + \left(\frac{g_{12}}{\omega_C} + \frac{2g_{12}C_s}{\omega_C C_{ab}}\right)(\epsilon\right. \end{array}\right.$$

$$\text{DENOMINATOR}$$

$$+ \left(\frac{\epsilon_o A}{2}\right)(4)(2V_{cr})^2 \left\{\frac{1}{(s_o - x)^2}\left[(\epsilon_o A)^2\left(\frac{1}{(s_o + x)^2}\right) + 2C_s(\epsilon_o A)\left(\frac{1}{(s_o + x)}\right) + \frac{g_{12}^2}{\omega_C^2} + C_s^2\right] - \frac{1}{(s_o + x)^2}\right.$$

$$\text{DENOMINATOR}$$

$$- \dot{x}(\epsilon_o A)^2 R_{12}\left(2V_{cr}V_B \frac{R_1}{R} \frac{R_2}{R}\right)\left\{\begin{array}{l} 2(R_e\mathfrak{F}_K + R_e\mathfrak{F}_V)\left[\frac{(\epsilon_o A)^3}{C_{ab}}\left(\frac{1}{(s_o - x)^2 (s_o + x)} - \frac{1}{(s_o - x)(s_o + x)^2}\right) + \left(1\right.\right. \\ - 2(I_m\mathfrak{F}_K + I_m\mathfrak{F}_V)\left[\left(\frac{g_{12}}{\omega_C C_{ab}}\right)(\epsilon_o A)^2\left(\frac{1}{(s_o - x)^2} - \frac{1}{(s_o + x)^2}\right) + \left(\frac{g_{12}}{\omega_C} + \frac{2g_{12}}{\omega_C}\right.\right. \end{array}\right.$$

$$\text{DENOMINATOR}$$

$$- \dot{x}(\epsilon_o A)^2 R_{12}(4)(2V_{cr})^2 \left\{\frac{1}{(s_o + x)^4}\left[(\epsilon_o A)^2\left(\frac{1}{(s_o - x)^2}\right) + 2C_s(\epsilon_o A)\left(\frac{1}{(s_o - x)}\right) + \frac{g_{12}^2}{\omega_C^2} + C_s^2\right] + \frac{}{(s\right.$$

$$\text{DENOMINATOR}$$

$$\text{DENOMINATOR} = \frac{(\epsilon_o A)^4}{C_{ab}}\left[\frac{1}{(s_o - x)^2 (s_o + x)^2}\right] + \left(\frac{2C_s}{C_{ab}^2} + \frac{2}{C_{ab}}\right)(\epsilon_o A)^3\left[\frac{1}{(s_o - x)^2 (s_o + x)} + \frac{1}{(s_o + x)^2 (s\right.$$

$$+ \left[\left(\frac{R_{12}^2}{\omega_C^2 C_{ab}^2} + \frac{C_s^2}{C_{ab}^2}\right)(2C_s) + (g_{12}^2 + C_s)\left(\frac{2}{C_{ab}}\right) + \frac{4C_s^2}{C_{ab}} + 4C_s\right](\epsilon_o A)\left[\frac{1}{(s_o - x)} + \frac{1}{(s_o + x)}\right]$$